Navigation Functions in Topologically Complex 3-D Workspaces

Savvas G. Loizou

Abstract— **Navigation Functions constructed according to the Koditschek-Rimon construction require the workspace to be topologically simple, i.e. homeomorphic to a sphere world. This paper proposes the first provably correct construction of Navigation Functions in 3D workspaces that are topologically complex. To achieve this construction, an extension of the recently introduced Navigation Transformation is proposed, that can handle any workspace and obstacle topology that can be categorized under the Classification Theorem of orientable 2-manifolds. The constructed Navigation Function is based on an underlying harmonic potential, that is guaranteed by construction to be free of local minima, hence tuning free in that aspect. In addition to the theoretical guarantees, a case study is presented along with a non-trivial computer simulation to demonstrate the effectiveness of the proposed solution.**

I. INTRODUCTION

Since the introduction of Navigation Functions in the early 90's by Koditschek and Rimon [7], [12], many extensions have appeared in the literature, to capture such features as systems with second order dynamics [12], non-holonomic systems [13], centralized multirobot systems [10] as well as decentralized systems [6] to mention a few.

More recently, an increased interest towards Micro Aerial Vehicles (MAV) [11], [3], motivated the problem of 3D Navigation in geometrically and at the same time topologically complex workspaces as these are encountered e.g. in indoor environments or in ruin sites in the context of urban search and rescue missions. Due to the reduced on-board computational capabilites of those systems, one needs efficient, closed form, fast feedback based navigation solutions, with guaranteed performance. This would have been just an appropriate domain for the application of traditional (i.e. according to Koditschek-Rimon construction) Navigation Functions, if it were not for the increased topological complexity encountered in the 3rd dimension. Unfortunately, except from special cases, 3-dimensional workspaces are not diffeomorphic to sphere worlds, hence the traditional Navigation Function machinery would have to sacrifice completeness (i.e. bound the non-sphere-diffeomorphic objects with sphere-diffeomorphic ones and in the process lose solutions) if it were to be applied. This paper proposes a solution to this problem by exploiting and appropriately extending the concept of the Navigation Transformation, proposed by the author in [8]. In a previous work a solution exploiting the Navigation Transformation for the 2-dimensional problem was proposed by the author in [9]; however the extension to

S.G. Loizou is with the Faculty of Mechanical Engineering and Materials Science and Engineering, Cyprus University of Technology, 45 Kitiou Kyprianou Str., Limassol 3041, CYPRUS savvas.loizou@cut.ac.cy

the 3-dimensional case is far from being a trivial task, since the topology in 3-dimensions is fundamentally different from the 2-D.

This paper presents the first to the author's knowledge provably correct Navigation Functions for 3-dimensional workspaces that are not homeomorphic to spheres. In a real-world robotic navigation problem, any possible workspace entity will occur as the boundary of some smooth solid object, that is a compact, connected, orientable 2-manifold. Under the view of the Classification Theorem of orientable 2-manifolds, all these entities are uniquely classified by their genus - a topological invariant. This paper utilizes this classification to completely capture any possible workspace geometry in 3-dimensions. In higher dimensions the problem becomes essentially more difficult. If fact it was shown that in 4 dimensions no algorithm classifying compact orientable manifolds is possible [4]. Hence the results presented in this paper are applicable assuming a diffeomorphism between every workspace entity and a model entity exists (something that is true for smooth solid objects). An appropriate model world -the *NT reference world*- is presented as the domain where the Extended Navigation Transformation maps the workspace. The motion and path planning problems can readily be solved with the proposed Extended Navigation Transformation according to the approach presented in [8] and are not presented in this paper. In this paper, in order to establish a dynamically sound and robust solution, a (locally) harmonic potential is installed on the *NT reference world* that is by construction free of local minima due the properties of harmonic functions. The Navigation Function is then constructed based on this (locally) harmonic function and a navigation vector field can be pulled back to the original workspace. The problem of systematically constructing of diffeomorphisms from the workspace to the *NT reference world* is not dealt with in the current paper. However a case study is presented.

The rest of the paper is organized as follows: Section II presents preliminary notions, while section III presents the Extended Navigation Transformation. Section IV presents the construction of Navigation Functions on the W_{NT} reference world. Section V presents simulation results on from a case study and the paper concludes with section VI.

II. PRELIMINARIES

In the following we will introduce the necessary terminology and definitions for the development of the methodology.

Let K be a set. Then $\overset{\circ}{K}$ denotes the interior of the set while ∂K denotes its boundary. $\mathcal{S}^n$ denotes the n-sphere.

The workspace $\mathcal{W} \subset \mathbb{E}^3$ is a compact connected smooth manifold with boundary.

A smooth version of the definition of a Navigation Function [7], is provided:

Definition 1: Let $\mathcal{W} \subset \mathbb{E}^n$ be a compact connected smooth manifold with boundary. A map $\varphi : \mathcal{W} \to [0,1]$, is a navigation function if it is:

1) Smooth on $\mathcal{W}$.
2) Polar on $\mathcal{W}$, with minimum at $q_d \in \overset{\circ}{\mathcal{W}}$.
3) Morse on $\mathcal{W}$.
4) Admissible on $\mathcal{W}$.

The following Classification Theorem is fundamental for 2-D manifolds:

Theorem 1: [4] Every compact, connected, orientable 2-manifold is homeomorphic to a sphere with handles added. Two such manifolds with the same number of handles are homeomorphic and conversely, so that the number of handles (called the genus) is the only topological invariant.

III. THE EXTENDED NAVIGATION TRANSFORMATION

A. The NT reference world

In order to define the Extended Navigation Transformation, we will first define the geometry of the image of a 3-D workspace under the transformation, the *NT reference world* - $\mathcal{W}_{NT}$.

An $\mathcal{W}_{NT}$ world is constructed by the following procedure:

1) **The external boundary of** $\mathcal{W}_{NT}$: Take a 3-ball $\mathbb{B} \subseteq \mathbb{R}^3$ with infinite radius and consider g_w non-intersecting parallel lines $L_1, \ldots L_{g_w}$. Define the set $B_{g_w} = \mathbb{B} \setminus \bigcup_{i=1}^{g_w} L_i$. The external boundary of $\mathcal{W}_{NT}$ is then constructed as

$$\mathcal{W}_{NTb} \triangleq B_{g_w} \setminus \overset{\circ}{B}_{g_w}$$

2) **Transformed Obstacles**: $\mathcal{W}_{NTb}$ partitions $\mathbb{R}^3$ in two sets: the external region E^+ and the internal region E^-. Obstacles are mapped to subsets of E^-. The obstacle set comprises the following:

 a) *Point Obstacles*: Take M_p discrete points p_i inside E^-. Then the i'th point obstacle is:

$$O_{pi} \triangleq p_i$$

 where $i = 1, \ldots M_p$. The set of all point obstacles is:

$$O_p \triangleq \bigcup_{i=1}^{M_p} O_{pi}$$

 b) *g-Torus Obstacles*: Take r_j 1-spheres $\mathcal{S}_i^1 \subset \overset{\circ}{B}_{g_w}$, $i = 1, \ldots r_j$ that form an open chain. For any $k, n \in \{1, \ldots r_j\}$, $\mathcal{S}_k^1$ intersects $\mathcal{S}_n^1$ at most at one point. Then the j'th g-Torus obstacle is constructed as

$$T_{g,j} = \bigcup_{i=1}^{r_j} \mathcal{S}_i^1$$

where $j = 1, \ldots M_g$, where M_g the number of g-Torus obstacles. Hence the boundary of obstacle $T_{g,j}$ is a torus of genus $g = r_j$. The set of all g-Torus obstacles is then:

$$T \triangleq \bigcup_{j=1}^{M_g} T_{g,j}$$

We can now construct the *NT reference world* as:

$$\mathcal{W}_{NT} = B_{g_w} \setminus (O_p \cup T)$$

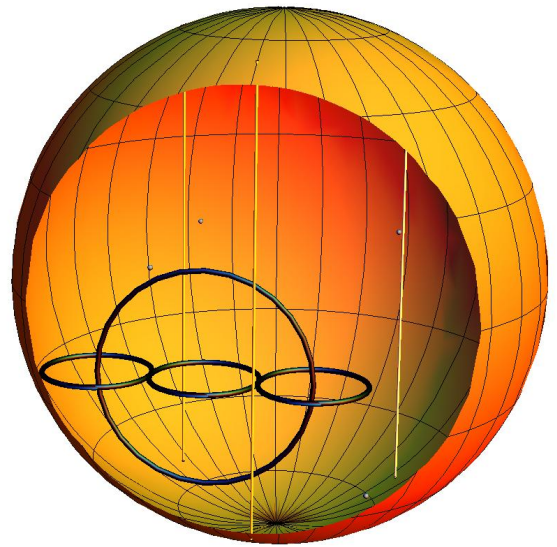An example of an *NT reference world* is depicted in Fig. 1.

Fig. 1. An example of an *NT reference world* with a genus–3 workspace boundary, 4 point obstacles, one 1-torus obstacle and one 3-torus obstacle

B. Definitions of the Extended Navigation Transformation and the valid workspace

We can now define the Extended Navigation Transformation:

Definition 2: The Extended Navigation Transformation is a diffeomorphism $\Phi_x : \overset{\circ}{\mathcal{W}} \to \overset{\circ}{\mathcal{W}}_{NT}$ that maps the workspace $\mathcal{W}$ to an *NT reference world*.

The valid workspace can now be defined as follows:

Definition 3: A workspace $\mathcal{W}$ is valid if it is diffeomorphic to $\mathcal{W}_{NT}$.

Note that a systematic construction of diffeomorphisms from a 3D worskpace to $\mathcal{W}_{NT}$ are beyond the scope of this paper. However section V presents a case study of such a transformation.

IV. Construction of a Navigation Function on $\mathcal{W}_{NT}$ based on Harmonic Potentials

A. Preliminaries

Assuming that the workspace has been diffeomorphically mapped to $\mathcal{W}_{NT}$, the construction of the navigation function is performed by first setting up a (locally) harmonic potential in $\mathcal{W}_{NT}$.

Let h be the robot's position in the $\mathcal{W}_{NT}$. We will now construct the harmonic potential contribution for each entity of $\mathcal{W}_{NT}$.

B. Harmonic Potential of a Line

Assume the i'th line passing from point l_i that is parallel to the vector n_l. Then the harmonic potential of a line in 3-D is provided as:

$$V_{l,i}(h) = -\ln \|(h - l_i) \times \hat{n}_l\|$$

where $i = 1 \ldots g_w$ and $\hat{n}_l = [0 \ 0 \ 1]$.

C. Harmonic Potential of a point

Assume point p_i. Then the harmonic potential from that point is:

$$V_{p,i}(h) = \frac{1}{\|h - p_i\|}$$

where $i = 1 \ldots M_p$

D. Harmonic Potential of a g-Torus obstacle

In order to create the harmonic potential of a g-Torus, we will assume a homogeneous distribution of harmonic potentials across its constituting circles.

Assume a circle $\mathcal{S}^1$ centered at point t_{ji}, lying on a plane perpendicular to vector n_{tji}, having a radius r_{ji}, with homogeneous harmonic potential distribution $dV = \frac{1}{d} \, ds$ where d is the distance between the infinitesimal potential distribution on the circle, and the point where the potential is evaluated.

Let

$$z_{ji}(h) \triangleq (h - t_{ji}) \cdot n_{tji}$$

and

$$\rho_{ji}(h) \triangleq \|(h - t_{ji}) \times n_{tji}\|$$

For notational brevity, indices will be omitted whenever possible. The potential induced at point h is:

$$V_{c,ji}(h) = \int_0^{2\pi} \frac{r}{\sqrt{z(h)^2 + \rho(h)^2 + r^2 - 2r\rho(h)\cos(\phi)}} \, d\phi$$

Substituting $\phi = \pi + 2\theta$ and setting:

$$\beta_{ji}(h) = \frac{4\rho_{ji}(h) r_{ji}}{z_{ji}(h)^2 + (\rho_{ji}(h) + r_{ji})^2}$$

Note that $0 \leq \beta_{ji}(h) < 1$. After some algebraic manipulation (see also [5]), we get:

$$V_{c,ji}(h) = \frac{4r_{ji}}{\sqrt{z_{ji}(h)^2 + (\rho_{ji}(h) + r_{ji})^2}} K[\beta_{ji}(h)]$$

where

$$K[m] = \int_0^{\pi/2} \frac{d\theta}{\sqrt{1 - m\sin^2(\theta)}}$$

with $K(m^2) = \mathcal{K}(m)$, is the complete elliptic integral of the first kind. Note the following:
1) $K[0] = \frac{\pi}{2}$
2) $\lim_{m \to 1} K[m] = \infty$

Since $V_{c,ji}(h)$ is an integral of a harmonic potential distribution, it will also be harmonic. The potential of the j-th g-Torus obstacle of genus g_j in $\mathcal{W}_{NT}$ is given as:

$$V_{t,j(h)} = \sum_{i=1}^{g_j} V_{c,ji}(h)$$

where $j = 1 \ldots N_T$ and N_T is the number of g-Torus obstacles.

E. Locally Harmonic Destination Potential

We note that a strictly increasing radial harmonic potential $V_d(h)$ with the property that $\lim V_d(h)_{h \to +\infty} = +\infty$ is not possible for dimensions higher than 2. Hence what is proposed here is a potential that is harmonic harmonic within a ball of radius d_{max}.

Without loss of generality, we assume that the destination configuration is the origin in $\mathcal{W}_{NT}$. Let $m_L = \arg\max_{i \in 1 \ldots g_w} \|(h_d - l_i) \times n_{li}\|$ be the index of the line that is farthest away from the destination configuration. Then the distance of this line from the destination configuration is $d_{l,max} = \|(h_d - l_{m_L}) \times n_{lm_L}\|$.

Let $m_p = \arg\max_{i \in 1 \ldots M_p} \|h_d - p_i\|$ be the index of the point that is farthest away from the destination configuration. Then the distance of this point from the destination configuration is $d_{p,max} = \|h_d - p_{m_p}\|$

Let $m_t = \arg\max_{ji} \|h - t_{ji}\|$ where $j \in 1, \ldots N_T$ and $i \in 1, \ldots g_j$, denote the index of the circle center that is farthest away from the destination configuration. Also let $m_r = \arg\max_{ji}(r_{ji})$ where $j \in 1, \ldots N_T$ and $i \in 1, \ldots g_j$, denote the index of the maximum radius of the circles constituting the g-Torus obstacles. Then define the indicative distance of the g-Torus obstacle from the destination configuration, as: $d_{t,max} = \|h - t_{m_t}\| + r_{m_r}$.

We can now define

$$d_{max} \triangleq 2\max\{d_{l,max}, \ d_{p,max}, \ d_{t,max}\} \tag{1}$$

.

Define the following smooth switch function:

$$\sigma(x) = \frac{s(x - d_{max})}{s(x - d_{max}) + s(\varepsilon - x + d_{max})}$$

Where
$$s(x) \triangleq \begin{cases} e^{-1/t} & t > 0 \\ 0 & t \leq 0 \end{cases}$$

and ε a small positive parameter defining the width of the transition band. Define the function:

$$v(x) = -\frac{K_1}{x}(1 - \sigma(x)) + (K_2 x^2 - K_3)\sigma(x)$$

The destination potential is then constructed as follows:

$$V_d(h) = v(\|h\|) \tag{2}$$

The choice of the destination potential motivates the following partitioning of $\mathcal{W}_{NT}$:

- The *harmonic domain*, $\mathcal{H} = \{h | \|h\| \leq d_{max}\}$
- The *transition band*, $\mathcal{T} = \{h | d_{max} < \|h\| < d_{max} + \varepsilon\}$
- The *radially unbounded domain* $\mathcal{R} = \{h | \|h\| \geq d_{max} + \varepsilon\}$

By construction $V_d(\cdot)$ is harmonic in $\mathcal{H}$. We have the following property for $V_d(\cdot)$:

Lemma 1:

$$\min_{h \in \{\mathcal{T} \cup \mathcal{R}\}} \|\nabla V_d(h)\| > \frac{K_1}{(d_{max} + \varepsilon)^2}$$

Proof: See section A in the Appendix ∎

Select $K_1 = G_{max}(d_{max} + \varepsilon)^2$, $K_2 = \frac{K_1}{2d_{max}^3}$ and $K_3 = K_2 d_{max}^2$. The constants are chosen to match the gradient and level of potential at d_{max}. By the choice of K_1, Lemma 1 becomes:

$$\min_{h \in \{\mathcal{T} \cup \mathcal{R}\}} \|\nabla V_d(h)\| > G_{max}$$

where G_{max} a constant that has to be appropriately chosen.

F. Construction of the Navigation Function

The (locally) Harmonic potential on $\mathcal{W}_{NT}$ is constructed as

$$\phi(h) = V_d(h) + \sum_{i=1}^{g_w} V_{l,i}(h) + \sum_{i=1}^{M_p} V_{p,i}(h) + \sum_{i=1}^{N_T} V_{t,i}(h) \tag{3}$$

Define the switch function

$$\sigma_e(x) \triangleq \frac{1}{2} + \frac{1}{2}\frac{x}{\sqrt{1 + x^2}}$$

that maps the extended real line to the interval $[0, 1]$. Define the following composition:

$$\Theta(\cdot) = \sigma_e \circ \phi \circ \Phi_x \tag{4}$$

We have the following results:

Lemma 2: There exists a bound $G_0 > 0$, such that all the critical points of ϕ lie inside the *harmonic domain*, $\mathcal{H}$ as long as $G_{max} \geq G_0$.

Proof: See section B in the Appendix. ∎

Corollary 1: There exists a constant $G_0 > 0$, such that $\Theta(\cdot) : \mathcal{W} \to [0, 1]$ is free of local minima as long as $G_{max} \geq G_0$.

Proof: Using Lemma 2, all the critical points of ϕ are in the harmonic domain and since ϕ is harmonic in $\mathcal{H}$ no critical point is a local minimum. Since Φ_x is a diffeomorphism, the result is inherited by Θ, as shown in the proof of Proposition 2.6 in [7]. ∎

The main result of the paper is the following:

Proposition 1: There exist a constant k_1, such that $\Theta(\cdot) : \mathcal{W} \to [0, 1]$ is a Navigation Function as long as $K_1 \geq k_1$

Proof: See section D in the Appendix. ∎

V. SIMULATION RESULTS

In order to demostrate the effectiveness of the proposed solution, a simulation has been setup in the Wolfram Mathematica 6.0 software. The workspace is depicted in figure 2.
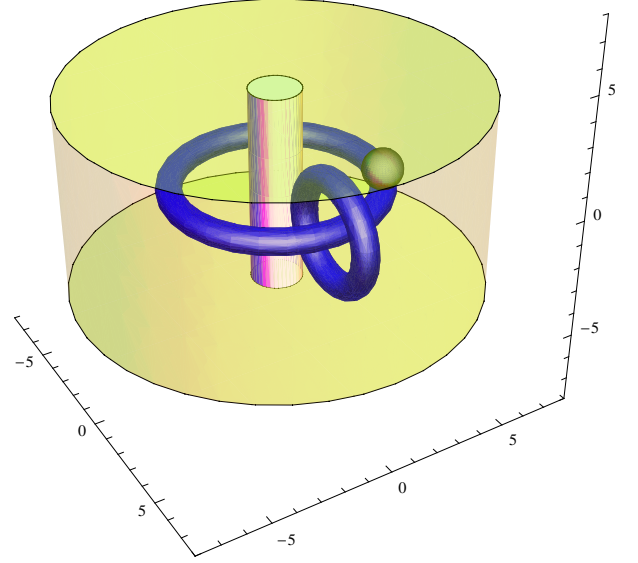

Fig. 2. Workspace with a genous-1 external workspace boundary, two 1-Torus obstacles and one spherical obstacle

A. Construction of Φ_x

In this section we provide an outline of the Extended Navigation Transformation that has been applied for the simulation for purposes of presentation completeness. The proof and the analysis of the implemented transformation are beyond the scope of this paper.

Define the following:

$$\eta(x) = \frac{s(x)}{s(x) + s(\delta - x)}$$

where δ is the activation distance. Define

$$\sigma_1(x) = \frac{x}{\delta}(1 + \eta(x)) + \eta(x)$$

Line transformation: First define the distance to the internal workspace cylindrical boundary as

$$b_l(q) = \|(q - p_l) \times n_l\| - r_w$$

where q is the robot position, p_l the cylinder's center and r_w the cylinder's radius. The distance to the sphere metric is defined as

$$b_s(q) = \|q - p_s\| - r_s$$

where p_s the sphere center and r_s its radius. The metric to the torus boundary for a torus centered at the origin is provided by the following:

$$b_t(q) = \left(R_t - \sqrt{q_x^2 + q_y^2}\right)^2 + q_z^2 - r_t^2$$

where R_t and r_t are the major and minor radii of the torus. A metric to the distance to the external workspace cylindrical boundary is provided by:

$$b_x(q) = r_x - \|(q - p_l) \times n_l\|$$

where r_x is the external workspace radius. A metric to the top and bottom surfaces of the workspace is provided by:

$$b_{wt}(q) = h_w - (q - p_l) \cdot n_l$$

Define the following transformations corresponding to the line, sphere, torus, external workspace cylinder, and top and bottom workspace bounding surfaces:

$$T_l(q) = (1 - \sigma_1(b_l(q)))((q - p_l) \times n_l) \times n_l$$

$$T_s(q) = (1 - \sigma_1(b_s(q)))(p_s - q)$$

$$T_t(q) = (1 - \sigma_1(b_t(q))) \cdot \ldots$$
$$\cdot \left(\frac{R_t(n_t \times (q - p_t) \times n_t)}{\|n_t \times (q - p_t) \times n_t\|} + p_t - q\right)$$

$$T_x(q) = (1 - \sigma_1(b_x(q)))(n_l \times (q - p_l) \times n_l)\frac{\delta}{b_x(q)}$$

$$T_{wt}(q) = (1 - \sigma_1(b_{wt}(q))) \cdot \ldots$$
$$\cdot ((q - p_l) \cdot n_l)\, n_l \frac{\delta}{h_w - \|q - p_l\| \cdot n_l}$$

Eventually the Extended Navigation Transformation is constructed as:

$$\Phi_x(q) = q + \sum_{i \in \{l, s, t_1, t_2, x, wt\}} T_i(q)$$

For the simulation we have implemented a system with dynamics:

$$\dot{x} = -\nabla\Theta$$

.

Figure 3 depicts the trajectory of the system under the influence of the negated gradient of the navigation function. As can be seen the trajectory of the system is safe - avoiding collisions with the obstacles and stable as expected.

Figure 4 offers another view of the same trajectory where the collision avoidance maneuver dictated by the flows of the navigation function can be seen.
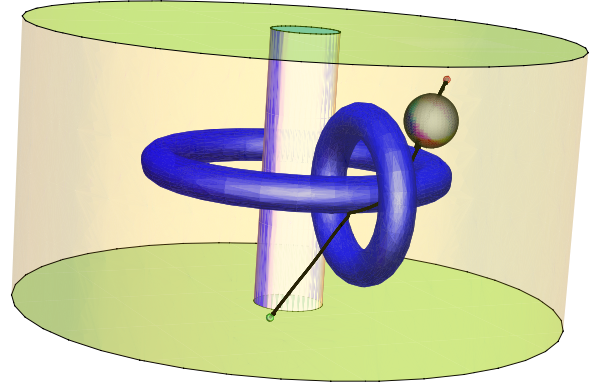

Fig. 3. Trajectory of a system with first order kinematics under the influence of the negated gradient of the Navigation Function. The green dot is the initial location and the red dot is the destination
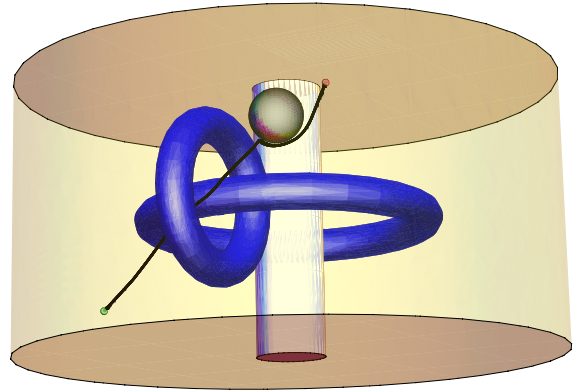

Fig. 4. Trajectory of a the simulation of the system from a different viewpoint

VI. CONCLUSIONS

In this paper a solution to the closed loop navigation in complex 3-D workspaces problem has been presented. The solution proposes a Navigation Function that is based on an underlying harmonic potential that is created on a model world where the Extended Navigation Transformation that is proposed in this paper has mapped the workspace. This is the first to the author's knowledge solution to the problem of constructing Navigation Functions on a 3-D topologies that can be categorized under the Classification Theorem of orientable 2-manifolds. Analytical guarantees are provided for the correctness of the proposed solution. A simulation of a case study is presented along with an outline suggestion for the construction of an Extended Navigation Transformation. In addition to the theoretical guarantees the simulation result demostrates the effectiveness of the proposed approach on a system with first order dynamics.

Further research includes developing a systematic approach to constructing the Extended Navigation Transformation, and apply the methodology to various systems, like aerial vehicles and underwater vehicles.

APPENDIX

A. Proof of Lemma 1

Proof: Assume a function

$$v_0(x) = f_1(x)(1 - \sigma(x)) + f_2(x)\sigma(x)$$

. Its derivative will be:

$$v_0' = (f_1'(1 - \sigma) + f_2'\sigma) + \sigma'(-f_1 + f_2)$$

. In our case $f_1(x) = -\frac{K_1}{x}$ and $f_2(x) = K_2 x^2 - K_3$.

Noting that $\sigma'(x) \geq 0$, all the terms are positive, assuming $K_2 d_{max}^2 - K_3 \geq 0$. By considering that the first part is a linear combination between the derivatives of f_1 and f_2 the value of v_0' is lower bounded by the lower value of either f_1 or f_2. However, since f_2 is convex, a conservative lower bound is given by f_1 at $d_{max} + \varepsilon$. Hence $\min_{h \in \{\mathcal{T} \cup \mathcal{R}\}} \|\nabla V_d(h)\| > \frac{K_1}{(d_{max}+\varepsilon)^2}$ ∎

B. Proof of Lemma 2

Proof: Assume that h is a critical point in $\mathcal{T} \cup \mathcal{R}$. Then

$$-\nabla V_d(h) = \sum_{i=1}^{g_w} \nabla V_{l,i}(h) + \sum_{i=1}^{M_p} \nabla V_{p,i}(h) + \sum_{i=1}^{N_T} \nabla V_{t,i}(h) \tag{5}$$

Let $\hat{u} = \frac{\nabla V_d}{\|\nabla V_d\|}$. Multiplying both sides of eq. (5) with $\hat{u}$, we get:

$$-\|\nabla V_d\| = \hat{u}U_l + \hat{u}U_R \tag{6}$$

where $U_l = \sum_{i=1}^{g_w} \nabla V_{l,i}(h)$ and $U_R = \sum_{i=1}^{M_p} \nabla V_{p,i}(h) + \sum_{i=1}^{N_T} \nabla V_{t,i}(h)$. Then according to Lemma 3:

$$U_R < U_{R,\max} = M_p p_0 + \sum_{j=1}^{M_g} r_j t_0$$

Create the following regions:

$$h : \|U_l\| < T_1$$

Then by choosing $\|\nabla V_d\|_{min} \geq 2T_1$ and $T_1 \geq U_{R,\max}$, equation (5) will not be satisfied in region 1 hence no critical points will be created there.

Region 2:

$$h : \|U_l\| \geq T_1$$

Multiplying both sides of eq. (5) with $\hat{n}_l$ we get:

$$-\hat{n}_l \nabla V_d = \hat{n}_l U_R \tag{7}$$

Note that

$$\|\nabla V_{l,i}(h)) = \frac{1}{\|(h - l_i) \times n_l\|}$$

Hence the cumulative line potential at a distance $\frac{\sqrt{2}}{2} d_{max}$ from the $\hat{n}_l$ axis will be at most:

$$U_{l,\sqrt{2}} = \frac{2g_w}{(\sqrt{2} - 1) d_{max}}$$

Hence requiring that $T_1 \geq U_{l,\sqrt{2}}$ and (from equation (7) that $\|\nabla V_d\| \geq \sqrt{2} \|U_R\|_{max}$ guarantees that equation (5) will not be satisfied in region 2.

Now in view of Lemma 1, the proof is completed by selecting $G_{\max} \geq G_0 = 2 \max \left\{ U_{R,\max}, \ U_{l,\sqrt{2}} \right\}$ ∎

C. Bounds on $\|\nabla V_{p,i}\|$ and $\|\nabla V_{t,i}\|$

Lemma 3: Let $h \in \mathcal{T} \cup \mathcal{R}$. Then it holds that:

$$\|\nabla V_{p,i}(h)\| < \frac{4}{d_{max}^2} = p_0 \tag{8}$$

$$\|\nabla V_{c,i}(h)\| < \frac{857}{d_{max}} = c_0 \tag{9}$$

Proof:

Case 1: Assume $h \in \mathcal{T} \cup \mathcal{R}$. According to eq. (1), we have that

$$\|\nabla V_{p,i}(h)\| = \frac{1}{\|h - p_i\|^2} < \frac{4}{d_{max}^2}.$$

Case 2: For $\|\nabla V_{c,i}(h)\|$ we have that:

$$\nabla V_{c,ji} = K[\beta_{ji}(h)] \nabla A_{ji}(h) + A_{ji}(h) \nabla K[\beta_{ji}(h)]$$

where

$$A_{ji}(h) = \frac{4r_{ji}}{\sqrt{z_{ji}(h)^2 + (\rho_{ji}(h) + r_{ji})^2}} < \frac{4}{3}$$

After some algebraic manipulation, we get:

$$\|\nabla A_{ji}(h)\| = \frac{4r_{ji}}{z_{ji}^2 + (\rho_{ji} + r_{ji})^2} < \frac{8}{9} \frac{1}{d_{max}}$$

and

$$\beta_{ji}(h) < \frac{8}{9}$$

Now since $\mathcal{K}[x]$ is strictly increasing for $x \in (0, 1)$, so will be $K[x]$. Hence the following bound is obtained:

$$K[\beta_{ji}(h)] < K[\frac{8}{9}]$$

Writing $\beta_{ji}(h) = \beta_{ji}(\rho_{ji}(h), z_{ji}(h))$, we get:

$$\nabla \beta(\rho, z) = -\frac{4r(-r^2 + \rho^2 - z^2)\nabla\rho + 8r\rho z \nabla z}{((r + \rho)^2 + z^2)^2}$$

where indices have been dropped for notational brevity. Taking the norm and majorizing the expression, we get:

$$\|\nabla \beta_{ji}(h)\| < \frac{152}{d_{max}}$$

Regarding $\nabla K[\beta(h)]$, we have:

$$\nabla K[\beta(h)] = \frac{E[\beta] - (1 - \beta)K[\beta]}{2\beta(1 - \beta)} \nabla\beta(h)$$

where $E[x^2] = \mathcal{E}[x] = \int_0^{\pi/2} \sqrt{1 - x^2 \sin^2(\theta)} d\theta$ is the complete elliptic integral of the second kind.

From [1], [2] we have that: $\frac{E[r^2]-(1-r^2)K[r^2]}{r^2}$ is strictly increasing for $r \in (0,1)$. Substituting $\beta = r^2$ we get that for $\beta \in (0,1)$, $\frac{E[\beta]-(1-\beta)K[\beta]}{2\beta(1-\beta)}$ will also be increasing as a product of increasing functions. Hence we have that:

$$\|\nabla K[\beta(h)]\| < \frac{1539}{2} \frac{\left(E[\frac{8}{9}] - \frac{1}{9}K[\frac{8}{9}]\right)}{d_{max}} < \frac{641}{d_{max}}$$

Hence we have that:

$$\|\nabla V_{c,i}(h)\| < \frac{1}{d_{max}} \left(\frac{8}{9}K[\frac{8}{9}] + \frac{4}{3}641\right) < 857\frac{1}{d_{max}} \quad \blacksquare$$

D. Proof of Proposition 1

Proof: Property 1 of Definition 1 is satisfied since all involved functions are analytic or smooth on $\mathcal{W}$.

Regarding Property 2, according to Lemma 2 all critical points will lie inside $\mathcal{H}$, where function ϕ is harmonic, by choosing $G_{max} \geq G_0$. Hence no local minima of ϕ can be created in the harmonic domain. Then according to Proposition 2.6 in [7] the composition $\varphi = \sigma_e \circ \phi$ will inherit the critical point characteristics of the harmonic function and will hence be free of local minima. ϕ is undefined at singular points but φ can be continuously extended to include the singular points where $+\infty$ is mapped to $+1$ and $-\infty$ is mapped to 0. So the continuously extended φ will have a minimum at the destination configuration. Since the destination confiuration is the unique singular point where $\phi \to -\infty$ then it will be the unique minimum of the continuously extended φ. Hence φ is polar.

Regarding Property 3: Assume that h is a critical point. Then from eq. (3) we have that at the critical point it will hold that:

$$-K_1\frac{\hat{h}}{\|h\|^2} = \sum_{a\in\{l,p,c\}}\sum_{b(a)}\nabla V_{a,b}(h)$$

where $b(l)$ runs from $1\ldots g_w$, $b(p)$ from $1\ldots M_p$ and $b(c)$ from $(1,1)\ldots(N_T, g_{N_T})$. As K_1 increases, the critical point will be moving towards the boundary of an obstacle. Assume that this obstacle has potential $V_{n,m}$. Then while K_1 can increase arbitrarily, only the norm of $\nabla V_{n,m}$ will increase whereas the gradients of the rest of the obstacles will remain bounded. Let us write the critical point condition in the following form:

$$-K_1\frac{\hat{h}}{\|h\|^2} = \nabla V_{n,m}(h) + R(h)$$

where $R(h)$ contains the bounded contributions. Taking the Hessian of $\phi(h)$, we have that:

$$\mathcal{H}_\phi = \mathcal{H}_{V_d} + \mathcal{H}_{V_{n,m}} + R'(h)$$

where $R'(h)$ contains the bounded contributions to the Hessian. Note that the Hessian of $\mathcal{H}_{V_d}$ of V_d has the following eigenvalues: $\lambda_1 = -\frac{2K_1}{\|h\|^3}$, and $\lambda_2 = \lambda_3 = \frac{K_1}{\|h\|^3}$.

We will study each obstacle type case individually:

Case 1: $V_{n,m}$ is the line potential $V_{l,i}$. Then

$$\|\nabla V_{l,i}\| = \frac{1}{\|(h - l_i) \times n_l\|}$$

The Hessian $\mathcal{H}_{V_{l,i}}$ of $V_{l,i}$ has eigenvalues: $\lambda_1 = 0$, $\lambda_2 = -\frac{1}{\|(h-l_i)\times n_l\|^2}$, $\lambda_3 = \frac{1}{\|(h-l_i)\times n_l\|^2}$ and let v_1, v_2, v_3 be the corresponding orthonormal eigenvectors.

As K_1 increases, so will $\frac{1}{\|(h-l_i)\times n_l\|}$ to maintain the critical point condition. However λ_2 and λ_3 will be increasing much faster (with the square of that rate). Now assume that for some K_1, $\mathcal{H}_\phi$ becomes degenerate. This implies that $v_i^T\mathcal{H}_\phi v_i = 0$ for some i. If $i = 2$ or 3, then by increasing K_1, the eigenvalues λ_2 and λ_3 will increase much faster and dominate, rendering $v_i^T\mathcal{H}_\phi v_i \neq 0$. If $i = 1$, then by increasing K_1, $v_1^T\mathcal{H}_{V_d}v_1$ will dominate rendering $v_i^T\mathcal{H}_\phi v_i \neq 0$. Let K_l be the minimum value of K_1, above which the Hessian $\mathcal{H}_\phi$ is not degenerate.

Case 2: $V_{n,m}$ is the point potential $V_{p,i}$. Then

$$\|\nabla V_{p,i}\| = \frac{1}{\|(h - p_i)\|^2}$$

The Hessian $\mathcal{H}_{V_{p,i}}$ of $V_{p,i}$ has eigenvalues: $\lambda_1 = \lambda_2 = -\frac{1}{\|h-p_i\|^3}$, and $\lambda_3 = \frac{2}{\|h-p_i\|^3}$ and let v_1, v_2, v_3 be the corresponding eigenvectors.

As K_1 increases, so will $\frac{1}{\|(h-p_i)\|^2}$ to maintain the critical point condition. However $\lambda_1,\ldots\lambda_3$ will be increasing much faster. Now assume that for some K_1, $\mathcal{H}_\phi$ becomes degenerate. This implies that $v_i^T\mathcal{H}_\phi v_i = 0$ for some i. By increasing K_1, the eigenvalues $\lambda_1\ldots\lambda_3$ will increase much faster and dominate, rendering $v_i^T\mathcal{H}_\phi v_i \neq 0$. Let K_p be the minimum value of K_1, above which the Hessian $\mathcal{H}_\phi$ is not degenerate.

Case 3: $V_{n,m}$ is the circle potential $V_{c,ji}$. Then

$$\nabla V_{c,ji} = K[\beta_{ji}]\nabla A_{ji} + A_{ji}K'[\beta_{ji}]\nabla\beta_{ji}$$

where A_{ji} is defined in the proof of Lemma 2, and the Hessian $\mathcal{H}_{V_{c,ji}}$ takes the form:

$$\mathcal{H}_{V_{c,ji}} = K'[\beta]\left(2\left(\nabla A\nabla^T\beta\right)_s + A\nabla^2\beta\right) + \ldots \\ + K[\beta]\nabla^2 A + AK''[b]\nabla\beta\nabla^T\beta$$

where $(A)_s = \frac{1}{2}(A + A^T)$ denotes the symmetric matrix. As can be seen from the plots in Fig. 5, $K'[x] > K[x]$ for $x > 0.8$ and $K''[x] > K'[x] > K[x]$ for $x > 0.5$.

As K_1 increases, β will be moving closer to 1 to maintain the critical point condition. Let $u = \hat{\nabla}\beta$. Now assume that for some K_1, $\mathcal{H}_\phi$ becomes degenerate. However there is a lower bound K_{c1} of K_1, such that for any $K_1 > K_{c1}$, we will have that $u^T\mathcal{H}_\phi u \neq 0$. This is due to the fact that the term containing $K''[\beta]$ will dominate. However this establishes that the rank of $\mathcal{H}_\phi$ is at least 2 (since ϕ is harmonic). To establish that $\mathcal{H}_\phi$ is full rank, we ne to show that $(u^\perp)^T\mathcal{H}_\phi u^\perp \neq 0$. Multiplying the critical point condition with $u^\perp$ we get:

$$-K_1\frac{\hat{h}u^\perp}{\|h\|^2} = K[\beta]\nabla Au^\perp + Ru^\perp \quad (10)$$
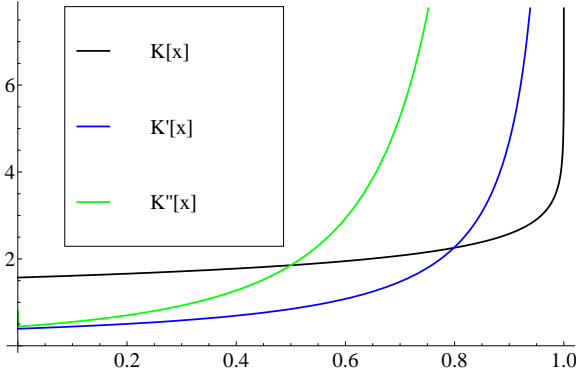
Fig. 5. Plot of the complete elliptic integral of the first kind $\mathcal{K}[\sqrt{x}]$ and it's first and second derivatives

Again as K_1 is increasing, β will be approaching to 1 to satisfy the critical point condition. Multiplying $\mathcal{H}_\phi$ with $u^\perp$, we get:

$$(u^\perp)^T \mathcal{H}_\phi u^\perp = (u^\perp)^T \left(\mathcal{H}_{V_d} + K'[\beta] A \nabla^2 \beta + \dots \right.$$
$$\left. \dots + K[\beta] \nabla^2 A + R \right) u^\perp$$

As K_1 increases, so will $K[\beta]$ to maintain the critical point condition eq. (10). However $K'[\beta]$ will be increasing much faster. Now assume that for some K_1, $(u^\perp)^T \mathcal{H}_\phi u^\perp = 0$. By increasing K_1, the term with $K'[\beta]$ will dominate[1] rendering $(u^\perp)^T \mathcal{H}_\phi u^\perp \neq 0$. Let K_{c2} be the lower bound of K_1 that $(u^\perp)^T \mathcal{H}_\phi u^\perp \neq 0$. Then requiring $K_1 \geq K_c = \max\{K_{c1}, K_{c1}\}$, the Hessian $\mathcal{H}_\phi$ is guaranteed to be non-degenerate.

To complete the Morse Property analysis we need to examine the destination configuration for non-degeneracy. Since the eigenvalues of $\mathcal{H}_{V_d}$ are $\lambda_\rho(\mathcal{H}_{V_d}) = \frac{K_1}{\|h\|^3}\{-2, 1, 1\}$, we can write

$$\mathcal{H}_\phi(h \to 0) = \frac{K_1}{\|h\|^3}\left(H_d + \|h\|^3 B \right)$$

where H_d and B are $O\left(\frac{1}{\|h\|}\right)$ matrices. Also note that

$$\nabla\phi(h \to 0) = -\frac{K_1}{\|h\|^2}\left(V_{d0} + \|h\|^2 V_{r0} \right)$$

where V_{d0} and V_{r0} are $O\left(\frac{1}{\|h\|}\right)$ vectors. Also

$$\phi(h \to 0) = \frac{K_1}{\|h\|}\left(1 + \|h\| \phi_{r0} \right)$$

where ϕ_{r0} is a $O\left(\frac{1}{\|h\|}\right)$ variable.

The Hessian of φ is

$$\mathcal{H}_\varphi = \sigma'_e(\phi) \mathcal{H}_\phi + \sigma''_e(\phi) \nabla\phi\nabla^T\phi$$

We have that

$$\sigma'_e(x) = \frac{1}{2}\frac{1}{(1+\phi^2)^{3/2}}$$

---

[1] Due to space constraints, linear independence of $\nabla\beta$ and $\nabla^2\beta u^\perp$ as well as the requirement that that $\nabla^2\beta \neq 0$ are placed as assumptions.

and

$$\sigma''_e(x) = -\frac{3}{2}\frac{\phi}{(1+\phi^2)^{5/2}}$$

Taking the limit as $h \to 0$ we get:

$$\mathcal{H}_\varphi(h \to 0) = \frac{1}{2K_1^2}\left(H_d - \frac{3}{K_1} V_{d0} V_{d0}^T \right)$$

However $V_{d0} V_{d0}^T = \hat{h}\hat{h}^T$ that is a single eigenvector matrix in the subspace spanned by the same eigenvector that corresponds to the eigenvalue $\lambda_1 = -2$ of H_d. Hence the effect of the last term would be to enhance this eigenvalue for the matrix $\mathcal{H}_\varphi$, that is thus guaranteed to be non-degenerate at the destination configuration. Choosing $K_1 \geq \max\{K_l, K_p, K_c\} = k_0$ completes the proof of the Morse Property.

Regarding Property 4: We have that $\partial \mathcal{W}$ is mapped to $\partial \mathcal{W}_{NT}$ by Φ_x. By construction $\phi(h \to \mathcal{W}_{NT}) = +\infty$ and $\phi(h \to \mathcal{W}_{NT}) = -\infty$. However function $\sigma_e(\cdot)$ maps $-\infty$ to 0 and $+\infty$ to 1, rendering $\Theta(\cdot)$ an admissible function.

The proof is completed by setting $k_1 = \max\{k_0, G_0(d_{\max} + \varepsilon^2)\}$.

∎

REFERENCES

[1] H. Alzer and S. Qiu. Monotonicity theorems and inequalities for the complete elliptic integrals. *Journal of Computational and Applied Mathematics*, 172(2):289–312, 2004.

[2] Glen D. Anderson, Mavina K. Vamanamurthy, and Matti K. Vuorinen. *Conformal Invariants, Inequalities, and Quasiconformal Maps*. John Wiley & Sons Inc., New York, 1997.

[3] M Bloesch, S Weiss, D Scaramuzza, and R Siegwart. Vision based mav navigation in unknown and unstructured environments. In *Proc. of The IEEE International Conference on Robotics and Automation (ICRA)*, May 2010.

[4] W. M. Boothby. *An Introduction to Differentiable Manifolds and Riemannian Geometry*. Academic Press Inc., 1986.

[5] Orion Ciftja, Arica Babineaux, and Nadia Hafeez. The electrostatic potential of a uniformly charged ring. *European Journal of Physics*, 30(3):623, 2009.

[6] D.V. Dimarogonas, S.G. Loizou, K.J. Kyriakopoulos, and M.M. Zavlanos. A feedback stabilization and collision avoidance scheme for multiple independent non-point agents. *Automatica*, 42(2):229–243, 2006.

[7] D. E. Koditschek and E. Rimon. Robot navigation functions on manifolds with boundary. *Advances Appl. Math.*, 11:412–442, 1990.

[8] S.G. Loizou. The navigation transformation: Point worlds, time abstractions and towards tuning-free navigation. *The 19th Mediterranean Conference on Control and Automation*, pages 303–308, 2011.

[9] S.G. Loizou. Closed form navigation functions based on harmonic potentials. *50'th IEEE International Conference on Decision and Control*, 2011(to appear).

[10] S.G. Loizou and K.J. Kyriakopoulos. Navigation of multiple kinematically constrained robots. *IEEE Transactions on Robotics*, 24(1):221–231, Feb. 2008.

[11] D. Mellinger and V. Kumar. Minimum snap trajectory generation and control for quadrotors. In *Proceedings of the IEEE International Conference on Robotics and Automation (ICRA)*, May 2011.

[12] E. Rimon and D. E. Koditschek. Exact robot navigation using artificial potential functions. *IEEE Trans. on Robotics and Automation*, 8(5):501–518, 1992.

[13] H. G. Tanner, S. G. Loizou, and K. J. Kyriakopoulos. Nonholonomic navigation and control of cooperating mobile manipulators. *IEEE Trans. on Robotics and Automation*, 19(1):53–64, 2003.